Functional Consequences of Lidocaine Binding to Slow-inactivated Sodium Channels

JEFFREY R. BALSER,‡ H. BRADLEY NUSS,* DMITRY N. ROMASHKO,* EDUARDO MARBAN,* and GORDON F. TOMASELLI*

*Section of Molecular and Cellular Cardiology, Department of Medicine, and the ‡Department of Anesthesiology and Critical Care Medicine, The Johns Hopkins School of Medicine, Baltimore, Maryland 21205

ABSTRACT Na channels open upon depolarization but then enter inactivated states from which they cannot readily reopen. After brief depolarizations, native channels enter a fast-inactivated state from which recovery at hyperpolarized potentials is rapid (<20 ms). Prolonged depolarization induces a slow-inactivated state that requires much longer periods for recovery (>1 s). The slow-inactivated state therefore assumes particular importance in pathological conditions, such as ischemia, in which tissues are depolarized for prolonged periods. While use-dependent block of Na channels by local anesthetics has been explained on the basis of delayed recovery of fast-inactivated Na channels, the potential contribution of slow-inactivated channels has been ignored. The principal (α) subunits from skeletal muscle or brain Na channels display anomalous gating behavior when expressed in *Xenopus* oocytes, with a high percentage entering slow-inactivated states after brief depolarizations. This enhanced slow inactivation is eliminated by coexpressing the α subunit with the subsidiary β_1 subunit. We compared the lidocaine sensitivity of α subunits expressed in the presence and absence of the β_1 subunit to determine the relative contributions of fast-inactivated and slow-inactivated channel block. Coexpression of β_1 inhibited the use-dependent accumulation of lidocaine block during repetitive (1-Hz) depolarizations from -100 to -20 mV. Therefore, the time required for recovery from inactivated channel block was measured at -100 mV. Fast-inactivated ($\alpha + \beta_1$) channels were mostly unblocked within 1 s of repolarization; however, slow-inactivated (α alone) channels remained blocked for much longer repriming intervals (>5 s). The affinity of the slow-inactivated state for lidocaine was estimated to be 15–25 μM, versus 24 μM for the fast-inactivated state. We conclude that slow-inactivated Na channels are blocked by lidocaine with an affinity comparable to that of fast-inactivated channels. A prominent functional consequence is potentiation of use-dependent block through a delay in repriming of lidocaine-bound slow-inactivated channels. Key words: sodium channel • slow inactivation • lidocaine • *Xenopus* oocytes • β_1 subunit

INTRODUCTION

Voltage-gated Na channels are pore-forming membrane proteins that are responsible for initiating action potentials in nerve, heart, and skeletal muscle. These channels assume a variety of conformational states depending on the transmembrane potential (Hodgkin and Huxley, 1952). At hyperpolarized membrane potentials, the channels reside in a rested, closed conformation. When the membrane potential is depolarized, the channels open briefly and then inactivate. Na channels cannot readily reopen from inactivated states, and they require recovery or "repriming" periods at hyperpolarized membrane potentials to regain availability.

Local anesthetics such as lidocaine act by blocking voltage-dependent Na channels. When hyperpolarized for long periods, Na channels exhibit a low affinity (>1 mM) for lidocaine. In contrast, high-affinity (10–100 μM) block is seen with repetitive depolarization, a phenomenon known as use dependence (Courtney, 1975). Use-dependent block is of critical importance since Na channels are subject to repetitive depolarization in excitable tissues. Use dependence has been attributed to an especially high affinity of the inactivated channel for lidocaine (Hille, 1977; Hondeghem and Katzung, 1977): Channels bind drug when they are depolarized and inactivated and then release drug when they are hyperpolarized and rested. Inactivated channels reprime far

Address correspondence to Jeffrey R. Balser, M.D., Ph.D., Department of Anesthesiology and Critical Care Medicine, The Johns Hopkins School of Medicine, Carnegie 442, 600 N. Wolfe St., Baltimore, MD 21287. Fax: (410) 955-7953; E-mail: jrbalser@welchlink.welch.jhu.edu

 J. GEN. PHYSIOL. © The Rockefeller University Press • 0022-1295/96/05/643/16 $2.00
Volume 107 May 1996 643–658

more slowly when associated with lidocaine; this delay in repriming contributes to use-dependent accumulation of block. Whereas the delay in repriming has been attributed to slow release of drug from a single inactivated state (Hille, 1977), many of the experimental results can be equally well explained by postulating the existence of drug-induced slow inactivated states with ultra-slow recovery kinetics (Khodorov et al., 1976).

In native tissues, drug-free Na channels can occupy at least two inactivated conformations that are kinetically distinct. Brief depolarizations induce fast inactivation, whereas prolonged depolarizations induce slow inactivation. Slow-inactivated channels require long (>1-s) repriming periods at hyperpolarized membrane potentials to recover from inactivation. In contrast, fast-inactivated channels require only brief (<20-ms) repriming intervals for recovery. Although the term slow inactivation can also be used to describe slow decay of the whole-cell Na current during a depolarizing step, we have restricted our use of the term to refer to a kinetically distinct inactivated state from which recovery is slow. This is the classical definition of slow inactivation originally proposed (Adelman and Palti, 1969; Chandler and Meves, 1970; Rudy, 1978) and subsequently adopted by others (Patlak, 1991). An advantage of this definition is that it focuses on the slow-inactivated state itself, rather than on the interesting but separate question of how that state may be entered. Although use dependence has been explained solely on the basis of delayed recovery of fast-inactivated Na channels from block (Hille, 1977), we considered the possibility that local anesthetic binding to the slow-inactivated state may significantly enhance use dependence. Unlike fast inactivation, which develops rapidly, slow inactivation requires many seconds to develop in native cells (Rudy, 1978), a feature that complicates simultaneous pharmacologic study of fast and slow inactivation. Nonetheless, slow inactivation merits attention because of its likely pathophysiologic importance in conditions where cells remain depolarized for long periods, such as ischemia.

Na channel α subunits, when expressed in *Xenopus* oocytes in the absence of the auxiliary β_1 subunit, conveniently display a prominent component of slow inactivation after short (<50-ms) depolarizations. Slow inactivation is markedly inhibited by coexpression of β_1 with the pore-forming α subunit. We examined the kinetics and steady-state properties of lidocaine block in *Xenopus* oocytes expressing skeletal muscle Na channel α subunits, with and without β_1. We find that coexpression of β_1 substantially attenuates use-dependent lidocaine block. The enhanced use dependence in the absence of β_1 is only partially explained by delayed repriming of the drug-associated fast-inactivated state. A prominent component of ultra-slow recovery was identified, and we argue that this results from lidocaine binding to the slow-inactivated state. Steady-state analysis indicated that slow-inactivated channels have a high affinity for lidocaine (15–25 μM), similar to that of fast-inactivated channels. We propose that both fast- and slow-inactivated states are blocked by low concentrations of lidocaine, and slow-inactivated channels exhibit ultra-slow unblocking properties, thus potentiating use-dependent block by lidocaine.

MATERIALS AND METHODS

Oocyte Expression

Plasmids encoding the rat skeletal muscle (μ1) α subunit were linearized with SalI, and the plasmids encoding rat brain β_1 subunit were linearized with EcoRI. Runoff cRNA transcription was performed using standard techniques (Backx et al., 1992). Oocytes were injected with 50 nl of 0.1–0.25 μg/μl solutions of cRNA containing either α subunit alone or a 1:1 mixture (by weight) of α and β_1 subunits. This ratio provides saturating β_1 effects on whole-cell current kinetics (Cannon et al., 1993). Oocytes were harvested from human chorionic gonadotrophin-primed adult female *Xenopus laevis* (Nasco, Ft. Atkinson, WI) using techniques described previously (Tomaselli et al., 1995). Oocytes were then stored in a modified Barth's solution containing (in mM): 88 NaCl, 1 KCl, 2.5 $NaHCO_3$, 15 Tris[hydroxymethyl] amino-methane, 0.4 $CaNO_3 \cdot 4\ H_2O$, 0.41 $CaCl_2 \cdot 6\ H_2O$, 0.82 $MgSO_4 \cdot 7\ H_2O$, 5 Na pyruvate, and 0.5 theophylline, and supplemented with 100 U/ml penicillin, 100 μg/ml streptomycin, 250 ng/ml fungizone, and 50 μg/ml gentamicin.

Electrophysiology and Data Analysis

Whole-cell currents were recorded 12–24 h after injection of cRNA using a two-microelectrode voltage clamp (OC-725B; Warner Instrument Corp., Hamden, CT). Electrodes were filled with 3 M KCl. Currents were sampled at 3–10 kHz (model TI-1 DMA Labmaster; Axon Instruments, Foster City, CA) and filtered at 1–2 kHz (−3 dB) with an eight-pole Bessel filter (Frequency Devices, Haverhill, MA). Currents were measured in solutions containing (in mM): 96 NaCl, 2 KCl, 1 $MgCl_2$, and 5 HEPES, pH 7.6. Lidocaine HCl (2% preservative free; Abbott Laboratories, North Chicago, IL) was added in appropriate amounts to give the concentrations indicated in figure legends. Currents were measured 10 min after addition of lidocaine to the bath. For dose-response measurements, oocytes were exposed to drug-free solutions and five incremental concentrations of lidocaine. With lidocaine present, intervals of at least 20 s at −100 mV were used to eliminate accumulation of block during voltage-clamp protocols. Acquisition and analysis of whole-cell currents was performed with custom-written software. Pooled data were expressed as means and standard errors, and statistical comparisons were made by one-way analysis of variance (ANOVA)[1] (Microcal Origin, Northampton, MA) or two-way ANOVA (SYSTAT for Windows, Evanston, IL).

[1] *Abbreviation used in this paper:* ANOVA, analysis of variance.

RESULTS

Effects of β_1 on Inactivation in Oocytes

Coexpression of the β_1 subunit is known to alter the gating kinetics of Na channels expressed in oocytes (Isom et al., 1992; Cannon et al., 1993; Bennett et al., 1993). Fig. 1 illustrates the profound changes in inactivation that occur when β_1 is coexpressed with μ1 Na channel α subunits. Currents through α subunits expressed alone decay slowly during a depolarizing clamp step; this decay is markedly accelerated by coexpression of the β_1 subunit (Fig. 1 *A*). Recovery from inactivation is also delayed when the β_1 subunit is omitted (Fig. 1 *B*). Channels were inactivated by depolarizing clamp steps to −20 mV, and recovery from inactivation was assessed by measuring the peak Na current during a subsequent test pulse to −20 mV after a repriming interval at −100 mV. For α subunits expressed alone and depolarized for 50 ms to −20 mV (*solid circles*), recovery was clearly biexponential and included a large slow component. After an initial rapid recovery phase representing Na channels recovering from fast-inactivated states, the remaining channels exhibited delayed recovery from slow-inactivated states (Zhou et al., 1991). Complete recovery at −100 mV required >5 s. The mean recovery data were fitted to a biexponential function (Fig. 1 legend); the slow component of the fit is shown by the dotted line (τ_2 = 2,061 ms).

Na channels composed of α + β_1 subunits subjected to the same 50-ms inactivating prepulse exhibited a much smaller slowly recovering component (*open circles*) (Cannon et al., 1993; Bennett et al., 1993; Zhou et al., 1991; Nuss et al., 1995*a*). The rapid component of recovery was increased in magnitude, but, like the α-alone channels, recovery was complete by 10 ms; we conclude that the rate of fast inactivation (τ_1 = 2.0 ms versus 2.8 ms for α alone) was not significantly altered by β_1 subunit coexpression. Similarly, while reduced in amplitude, the slow component of recovery was well fitted with the same time constant (τ_2 = 2,061 ms) as in channels without β_1 coexpressed, suggesting that recovery from the slow-inactivated state is not kinetically altered by β_1. Slow recovery of α + β_1 channels after prolonged 2-min depolarizing prepulses was also measured after 100- and 1,000-ms recovery periods at −100 mV (*open triangles*); these recovery data were also well fitted by the same time constant (2,061 s, *dotted line*). To illustrate this point more clearly, Fig. 1 *C* shows the normalized slow recovery data from 40 to 5,000 ms for all three cases considered in Fig. 1 *B*. The superimposed dotted line represents a single exponential function with a time constant of 2,061 ms, as determined from the fit to the α alone data in Fig. 1 *B*. The normalized slow recovery of α alone channels (*solid circles*) and α + β_1 channels after brief (*open circles*) or prolonged (*open tri-*

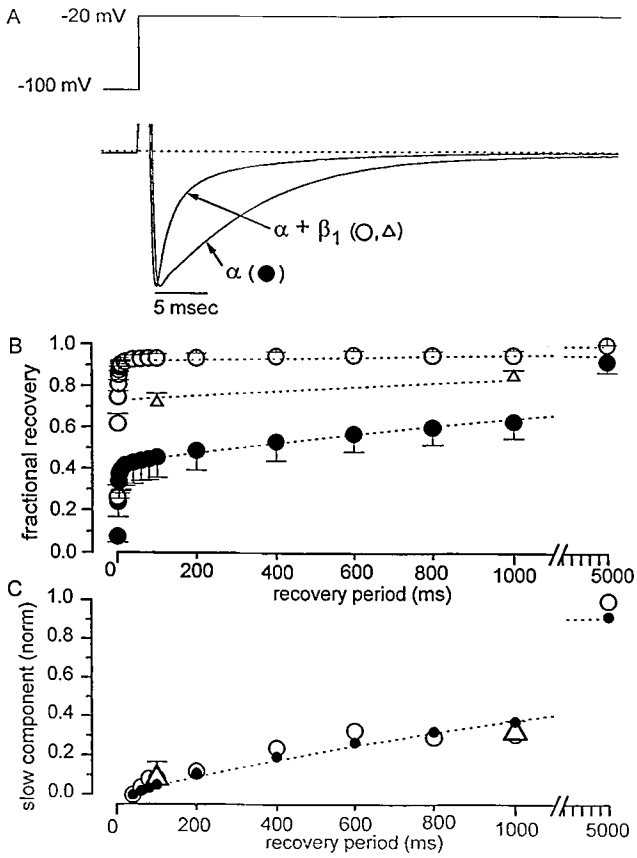

FIGURE 1. The effects of β_1 subunit coexpression on whole-cell Na current kinetics. (*A*) Comparison of whole-cell Na current decay in the absence and presence of the β_1 subunit. *Xenopus* oocytes were clamped to −20 mV for 50 ms, and inward currents were recorded. Currents were sampled at 100 μs and filtered at 2 kHz. Traces are scaled so that the peak amplitudes superimpose but are not leak subtracted. (*B*) Recovery from inactivation in the absence and presence of β_1. Channels were depolarized to −20 mV (P1) and then allowed to recover for variable test intervals at −100 mV (*abscissa*). The peak inward current measured during the subsequent test pulse (P2) was plotted relative to its fully available reference current as P2/P1. Solid circles (●) show currents measured in the absence of β_1 (six oocytes) after 50-ms P1 pulses. The open circles (○) show the results from oocytes expressing α + β_1 after the same 50-ms P1 pulses (nine oocytes). The open triangles (△) show currents results from oocytes expressing α + β_1 after a 2-min depolarizing P1 pulse (three oocytes). Dotted lines represent the slow (τ_2) component obtained by nonlinear least-squares fits of the biexponential function $y = A[1 + \exp(-t/\tau_1)] + B[1 + \exp(-t/\tau_2)]$ to the mean recovery data. For α alone, the fitted parameters were as follows: A = 0.42, B = 0.58, τ_1 = 2.8 ms, τ_2 = 2,061 ms. For α + β_1 after a 50-ms prepulse, the fitted parameters were as follows: A = 0.92, B = 0.08, τ_1 = 2.0 ms; the value of τ_2 was fixed (2,061 ms). Similarly, for α + β_1 after a 2-min prepulse, the fitted parameters were as follows: A = 0.73, B = 0.27, τ_1 = 2.8 ms; the value of τ_2 was again fixed (2,061 ms). (*C*) Data from *B* were normalized and plotted over the slow recovery interval from 40 to 5,000 ms. The same symbol conventions as in *B* are used. An increasing single-exponential function with a τ = 2,061 ms is superimposed (*dotted line*).

angles) depolarizations were similar and were well fitted by the same time constant, indicating the slow-inactivated state is kinetically similar in all three cases. These data suggest that α subunits expressed alone produce channels that enter the slow-inactivated state much more rapidly than do α + β_1 channels, but the properties of the slow-inactivated state are the same whether or not β_1 is coexpressed.

Use-dependent Block by Lidocaine Is Attenuated by β_1 Subunit Coexpression

Fig. 2 *A* shows the effects of lidocaine during a 1-Hz train of 50-ms depolarizations from −100 to −20 mV. The peak whole-cell Na currents are normalized to the current measured during the first pulse (I_1) and are plotted as a function of the pulse number. Steady-state reduction of the peak Na current developed rapidly and was measured at the eighth pulse (I_8). In the absence of drug, there was no reduction in the steady-state current with successive pulses for α + β_1 channels (*left, open circles*, $I_8/I_1 = 0.98 \pm 0.01$); however, for α alone (*right, open squares*) there was a substantial reduction in steady-state current because of incomplete recovery from inactivation between pulses ($I_8/I_1 = 0.69 \pm 0.07$). Lidocaine (*solid symbols*) produced a small use-dependent reduction of the current generated by α + β_1 channels (*left*, $I_8/I_1 = 0.90 \pm 0.03$). A much more substantial use-dependent reduction in Na current was seen in lidocaine-exposed oocytes expressing α alone (*right*, $I_8/I_1 = 0.25 \pm 0.11$). Two-way analysis of variance indicated that, in the absence of β_1, there was a significant increase in use-dependent block by lidocaine ($P < 0.05$ for lidocaine and β_1 interaction).

Studies of state-dependent block of Na channels by

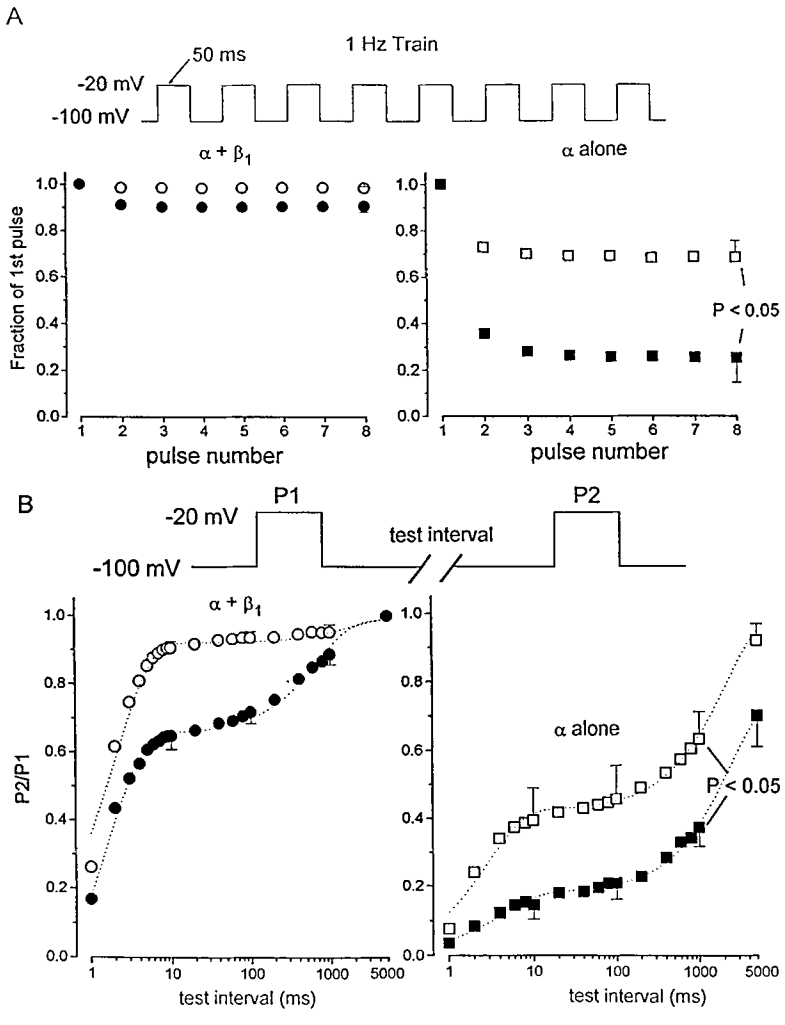

FIGURE 2. Use-dependent and inactivated-state block by lidocaine. (*A*) Channels were depolarized for 50 ms from −100 to −20 mV at a rate of 1 Hz. Peak Na currents were normalized to the current elicited by the first pulse in the train. Open symbols show drug-free control data for α + β_1 (*left, circles*, $n = 8$) and α alone (*right, squares*, $n = 4$). Solid symbols show currents measured in 174 μM lidocaine for α + β_1 (*left*, $n = 10$) and α alone (*right*, $n = 4$). The use-dependent reduction in current reached steady state rapidly and was measured at the eighth pulse in each train. For α + β_1, lidocaine reduced the steady-state peak Na current from 0.98 ± 0.01 to 0.90 ± 0.03. For α alone, lidocaine reduced the currents to a greater degree, from 0.69 ± 0.07 to 0.25 ± 0.11 ($P < 0.05$, two-way ANOVA). (*B*) Recovery from both inactivation and inactivated-state lidocaine block. Drug-free data are replotted from Fig. 1 *B* on a logarithmic scale to show the kinetic components of recovery. After 50-ms prepulses to −20 mV (*P1*), channels were allowed to recover at −100 mV for variable intervals. Fractional recovery, assessed by a second 50-ms pulse to −20 mV (*P2*), was plotted as P2/P1. Control data (*open symbols*) are from nine oocytes expressing α + β_1 (*left, circles*) and six oocytes expressing only the α subunit (*right, squares*). Experiments were performed with bath concentrations of 174 μM lidocaine (*solid symbols*) and include seven oocytes expressing α + β_1 (*left*) and six oocytes expressing only α (*right*). The dotted lines are the nonlinear least-squares fits of two exponentials to the mean data. Fitted parameters for control data are given in Fig. 1 *B*. For α subunits expressed alone, fractional recovery at 1 s in lidocaine was significantly reduced compared with drug-free solutions (37 ± 6% versus 63 ± 8%, $P < 0.05$). Lidocaine did not significantly reduce the fractional recovery at 1 s in α + β_1 channels (drug free 95 ± 2% versus 89 ± 3% in lidocaine). The fitted time constants for the slow components in the presence of drug (*dotted lines*) were 703 ms (α + β_1) and 2,400 ms (α alone).

local anesthetics suggest that lidocaine has a particularly high affinity for inactivated channels. The apparent increase in use-dependent block in the absence of β_1 may therefore relate to the delayed recovery from inactivation exhibited by these channels. To test this hypothesis in detail, we examined recovery from lidocaine block after a 50-ms inactivating prepulse in a manner identical to Fig. 1 *B*. Fig. 2 *B* shows the drug-free recovery from inactivation (*open symbols*) from Fig. 1 *B* replotted on a log axis to emphasize the kinetics of recovery. More than 90% of the $\alpha + \beta_1$ channels (*left*) recover within 10 ms at −100 mV, and only a small residual component recovers slowly. The principal kinetic component reflects channels recovering from fast-inactivated states. In the absence of β_1 (*right*), ~40% of the channels recover with the same rapid time course as $\alpha + \beta_1$. The remainder of the channels recover slowly, with a time constant of 2,061 ms. In summary, after a 50-ms depolarization to −20 mV, ~40% of the α-alone channels recover from fast-inactivated states, while the remainder recover from slow-inactivated states.

The addition of lidocaine reveals new kinetic components associated with recovery from inactivated-channel block (Fig. 2 *B*, *solid symbols*). The data are plotted as peak current measured during the test pulse (*P2*) relative to that elicited by the 50-ms inactivating pulse (*P1*), thereby eliminating the effect of rested or "tonic" block. For $\alpha + \beta_1$ channels (*left, filled circles*), 65% were not blocked and therefore recovered rapidly (<10 ms). The remaining blocked channels recovered with a mean time constant of 703 ms; ~90% of all channels had recovered by 1 s at −100 mV. In contrast, the α-alone channels (*right, solid squares*) exhibited an initial small, rapid component (~15%) associated with recovery of drug-free fast-inactivated channels. This was followed by a large slow component of recovery with a mean time constant of 2,400 ms. Whereas this component certainly includes fast-inactivated channels recovering from block, the slowed recovery relative to $\alpha + \beta_1$ suggests the presence of an additional blocked state. Since nearly 60% of the α-alone channels were slow inactivated in the absence of drug, lidocaine binding to the slow-inactivated state is likely. If so, the repriming of drug-bound slow-inactivated channels could logically be predicted to introduce an ultra-slow component of recovery. In agreement with that prediction, recovery from lidocaine block in the presence of slow inactivation (α alone) was far slower than in its absence ($\alpha + \beta_1$). Fractional recovery after 1 s in α-alone channels was significantly reduced by lidocaine (63 ± 8% in drug-free solutions versus 37 ± 6% in lidocaine, $P < 0.05$), but this was not the case in $a + \beta_1$ channels (drug free 95 ± 2% versus 89 ± 3% in lidocaine, $P = 0.1$). Thus, drug-exposed channels lacking the β_1 subunit display a large additional component of slowly recovering current consistent with lidocaine binding to slow-inactivated channel states. Alternatively, if the β_1 subunit accelerates recovery from fast-inactivated channel block, a more slowly recovering block component would be expected for α subunits expressed alone.

To discriminate between these two possibilities, we determined whether recovery from fast-inactivated channel block was slowed in the absence of β_1. To address this, it was necessary to identify a voltage-clamp protocol that would induce measurable fast inactivation, but little slow inactivation, in oocytes expressing α alone. First, the rate of development of slow inactivation for drug-free channels in the absence of β_1 subunit was examined (Fig. 3 *A*). Oocytes were clamped at −20 mV for variable periods and were then allowed to recover for 100 ms at −100 mV; fractional recovery from block was assayed by a subsequent test pulse to −20 mV. In drug-free conditions after a 50-ms depolarizing pulse, slow inactivation persisted well beyond 100 ms, whereas fast-inactivated channels recovered in <10 ms (cf. Fig. 2 *B*, *right*). We therefore used a 100-ms recovery interval to assay the time course of development of slow inactivation. Fig. 3 *A* shows that the time course of development of slow inactivation was sigmoidal. Fractional recovery at 100 ms after a 5-ms depolarization was 93 ± 1% ($n = 3$); hence, very little slow inactivation was induced by these brief depolarizing prepulses (Fig. 3 *A*).

The sigmoidal development of slow inactivation in oocytes expressing α subunits alone enabled us to use short depolarizing prepulses to elicit fast, but very little slow, inactivation. These voltage-clamp protocols facilitated measurement of recovery from fast-inactivated channel block in the absence of β_1. Fig. 3 *B* shows recovery from inactivation for α subunit channels in the absence of β_1 after 3-ms prepulses to −20 mV. Drug-free and lidocaine data are from the same oocyte. Fractional recovery from fast-inactivated channel block (*solid squares*) reached drug-free control (*open squares*) levels in ≤1 s (91 ± 2% recovery, $n = 3$). This rate of recovery from lidocaine block was not different ($P = 0.63$) from that observed in oocytes expressing $\alpha + \beta_1$ channels with 50-ms prepulses to −20 mV (Fig. 2 *B*, *left*; 89 ± 3% recovery by 1 s at −100 mV). Further, recovery after these brief prepulses was much faster than that associated with slow inactivation in α-alone channels in the absence of drug (cf. Fig. 2 *B*, *right*). We conclude that the β_1 subunit does not alter the rate of recovery from fast-inactivated state block, and the additional slowly recovering current in the absence of β_1 likely reflects lidocaine binding to slow-inactivated channel states.

The Affinities of Fast- and Slow-inactivated Channels for Lidocaine

Measuring the state-specific affinities of local anesthetics is inherently difficult since the resting state, the in-

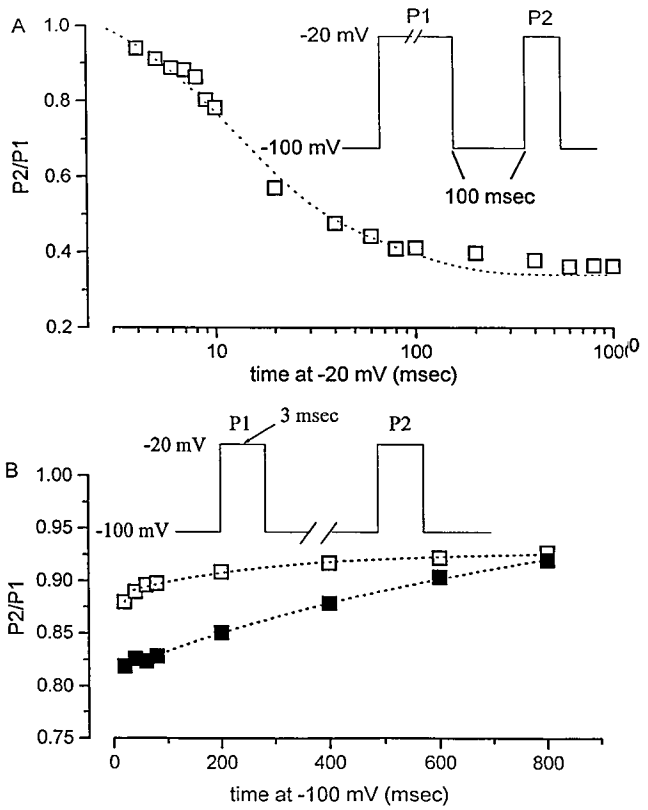

FIGURE 3. The time course of development of slow inactivation and recovery from fast-inactivated channel block in α-alone channels. (*A*) Under drug-free conditions, α-alone channels were depolarized to −20 from −100 mV for variable intervals from 3 to 1,000 ms (*P1*), and were then allowed to recover for 100 ms at −100 mV. The peak current measured during a subsequent test pulse to −20 mV (*P2*) is plotted relative to P1 to indicate fractional recovery from inactivation. Because the length of the recovery interval was >10 ms (adequate time for full recovery from fast inactivation), the time-dependent decrease in fractional recovery reflects the time course of development of slow inactivation. The time course of development of slow inactivation was sigmoidal, and fitting these data required a function with at least two exponentials (*dotted line*: A_1, τ_1, = 0.44, 12 ms; A_2, τ_2 = 0.21, 72 ms). (*B*) Recovery from fast inactivation and fast-inactivated channel block. Channels are depolarized for 3 ms at −20 mV (*P1*), and the fractional recovery (*P2/P1* at −20 mV) after periods from 20 to 800 ms at −100 mV is plotted. Open symbols indicate drug-free control data, and solid symbols show data from the same oocyte collected in 174 μM lidocaine. Fast-inactivated α-alone channels exhibited recovery from block after 1 s at −100 mV that was not different ($P = 0.63$) from α + β_1 channels recovering from fast-inactivated channel block (Fig. 2 *B*).

activated states, and all drug-bound states are nonconducting. Steady-state inactivation curves reflect the availability of Na channels to open as a function of membrane potential. Local anesthetic agents typically shift the steady-state inactivation curve to more negative membrane potentials because of the formation of drug-associated states that reduce channel availability for opening. However, at intermediate membrane potentials (−90 to −50 mV), channels are distributed among rested and inactivated states. The steady-state inactivation curve thus reflects drug association with multiple nonconducting states, complicating the relationship between drug affinity and the drug-induced voltage shift. A model-dependent method has therefore been used to determine the affinity of lidocaine for the rested and inactivated channel conformations (Bean et al., 1983). If lidocaine binds primarily to one of two nonconducting states, rested (*R*) or fast-inactivated (I_F), the shift in the inactivation curve reflects the relative partitioning between two drug-bound states (RL, I_FL).

$$\begin{array}{ccccc} R & \rightleftharpoons & O & \rightleftharpoons & I_F \\ \Updownarrow & & & & \Updownarrow \\ RL & & & & I_F L \end{array} \qquad (1)$$

In this model, the open state (O) is only transiently occupied. Whereas open-state block may influence use-dependent block (Matsubara et al., 1987; Makielski et al., 1991), we have assumed that any contribution to steady-state block is negligible. Our justification for exclusion of open-channel block is considered in greater detail below.

We used this simplified modulated-receptor model to determine the affinity of lidocaine for the fast-inactivated state using α + β_1 channels. First, we determined the length of depolarization necessary for fast-inactivated channels to equilibrate with drug, but not slow inactivate. To assess this, an oocyte expressing α + β_1 channels was clamped to −20 mV for variable time intervals (50–5,000 ms). Channels were then allowed to recover for 100 ms at −100 mV before a depolarizing test pulse to −20 mV. After 100 ms at −100 mV, drug-free channels should recover fully from fast inactivation, while very little recovery from fast-inactivated channel block will occur (cf. Fig. 2 *B*, *left*). Fig. 4 plots the fraction of inactivated channels in the absence of drug (*open squares*) and the fraction of inactivated and blocked channels in lidocaine (*solid circles*) as a function of the inactivating prepulse duration (*P1*). The fraction of unavailable channels in drug-free conditions was small, and represents the development of slow inactivation by α + β_1 channels over 5 s. The much larger fraction of unavailable channels in lidocaine therefore results primarily from fast-inactivated channel block, but to a small degree includes slow inactivation. The lidocaine data were well fitted to a biexponential function (*dotted line*) with a rapid large component (τ = 53 ms) that describes the time dependence for development of fast-inactivated channel block. In three such experiments with oocytes expressing α + β_1 channels, the time constant for development of fast-

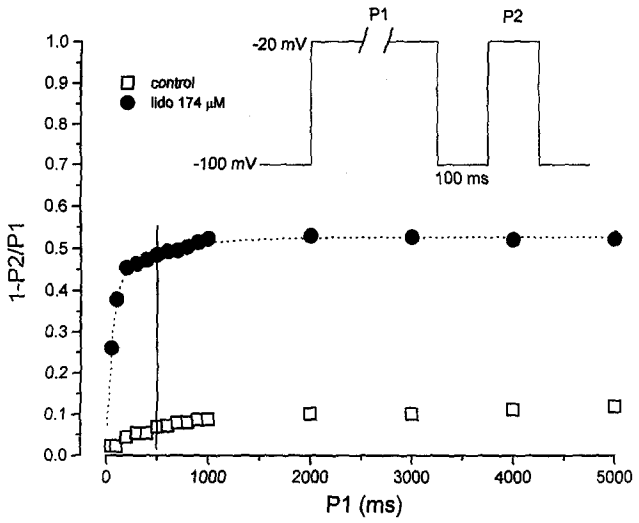

FIGURE 4. Time-course of development of fast-inactivated channel block in $\alpha + \beta_1$ channels. Peak inward current during a test pulse (*P2*) was measured after inactivating prepulses of varying duration (*P1*) at −20 mV. An intervening 100-ms recovery interval at −100 mV allowed full recovery of drug-free fast-inactivated channels without significant recovery of drug-bound fast-inactivated channels or slow-inactivated channels (see Fig. 2 *B*). The fraction of channels unavailable to open (*1 − P2/P1*) is plotted against the inactivating prepulse duration (*P1*). Control data (*open squares*) and data obtained during exposure to lidocaine (174 μM; *solid circles*) are shown for the same oocyte. An exponential function with two time constants was fitted to the lidocaine data (τ_1, τ_2 = 53, 503 ms). By 500 ms (*vertical line*), steady-state block of fast-inactivated channels is fully developed with minimal superimposed slow inactivation.

inactivated channel block was 86 ± 47 ms. Hence, fast-inactivated channel block was fully developed by 500 ms at −20 mV (*solid vertical line*, Fig. 4). Further, the control data (*open squares*) show that only ~7% of the channels slow inactivated during a 500-ms step to −20 mV. Therefore, 500-ms depolarizing prepulses were used to measure steady-state block of fast-inactivated $\alpha + \beta_1$ channels by lidocaine (Fig. 5).

In Fig. 5, oocytes expressing $\alpha + \beta_1$ channels were clamped to membrane potentials from −110 to −30 mV for 500 ms (*P1*). A subsequent test pulse to −20 mV (*P2*) assayed the fraction of channels available to open (residing in R state, Eq. 1). Fig. 5 *A* plots the peak Na currents recorded from a representative oocyte as a function of the P1 potential under drug-free conditions (*squares*) and during exposure to five concentrations of lidocaine. Currents at each concentration of drug were fitted to the Boltzmann equation. In drug-free conditions, $V_{1/2}$ was −50 ± 3 mV (n = four oocytes). Fig. 5 *B* shows the difference between the fitted $V_{1/2}$ at each drug concentration and the control $V_{1/2}$ ($V_{1/2}$ shift) measured in the same oocyte. A function, derived from the model given in Eq. 1 (see Bean et al., 1983 and Appendix) was fitted to these data to estimate the affinity of lidocaine for the rested state (K_R) and the fast-inactivated state (K_{IF}):

$$V_{1/2}\ \text{shift} = k \ln\ [(1 + [L]/K_R)\ (1 + [L]/K_{IF})^{-1}]. \quad (2)$$

In this equation, k is the mean slope from the fitted steady-state inactivation curves at each drug concentration $[L]$, whereas K_{IF} and K_R are the respective affinities of the fast-inactivated and rested states for lidocaine. The k from 18 Boltzmann fits to data from $\alpha + \beta_1$ channels was 5, similar to the value previously measured for cardiac Na channels (Bean et al., 1983); this value was used as a fixed parameter. Eq. 2 provided a good fit to the $V_{1/2}$ shift data (Fig. 5 *B*, *dotted line*) with an estimated K_{IF} of 24 μM and a K_R of 1,470 μM. As discussed below, these results compare favorably with those measured previously in cloned skeletal muscle Na channels (Nuss et al., 1995*b*) and native cardiac Na channels (Bean et al., 1983).

To incorporate steady-state block of α subunits expressed alone by lidocaine, we considered the potential contribution of the slow-inactivated channel. Single-channel data suggest that modal gating influences Na channel inactivation (Moorman et al., 1990; Ukomadu et al., 1992; Zhou et al., 1991). That is, long periods of quiescence thought to represent slow inactivation were temporally associated with a lower frequency gating mode that included bursting behavior (mode 2). However, the possibility that channels gating in the high frequency nonbursting mode (mode 1) may also slow inactivate, albeit on a longer time scale, was not excluded. Similarly, long quiescent periods in single-channel experiments with $\alpha + \beta_1$ channels are not consistently associated with mode 2 gating behavior (unpublished observations). If channels are able to slow inactivate from either gating mode, a single model with only a limited number of alterations in rate constants underlying the gating mode transitions may suffice to explain our data (Bennett et al., 1993). This general idea is exemplified by the following gating scheme, where I_F and I_S represent fast- and slow-inactivated states, respectively:

$$R \underset{k_2}{\overset{k_1}{\rightleftarrows}} O \underset{k_4}{\overset{k_3}{\rightleftarrows}} I_F \rightleftarrows I_S \quad (3a)$$

In both modes, if the recovery rate constant k_4 were very small, I_S would have a slow-inactivated character. In mode 1 the magnitude of the rate constants leaving I_F (k_2 and k_3) may also be small during depolarization, thereby "locking" channels in I_F after a single opening and preventing them from progressing to I_S unless depolarization is prolonged (as for the 2-min depolariza-

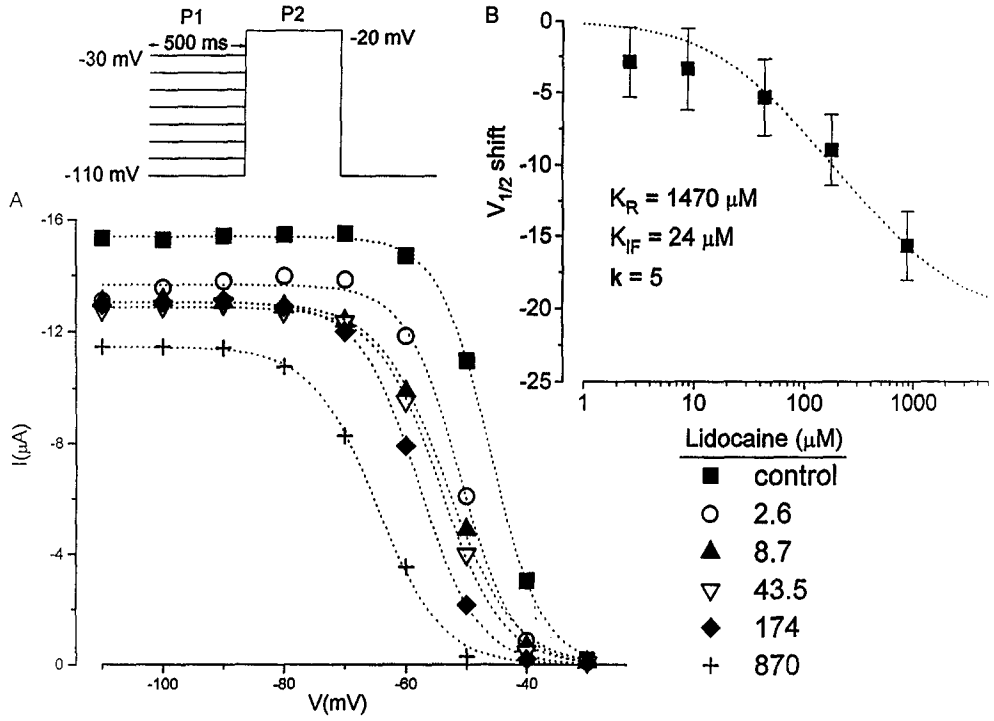

FIGURE 5. Steady-state block of fast-inactivated Na channels. Oocytes expressing α + β_1 channels were clamped to membrane potentials from −110 to −30 mV for 500 ms (*P1*). A subsequent test pulse to −20 mV (*P2*) was used to assess the number of channels available to open. (*A*) The peak Na currents recorded from a representative oocyte are plotted as a function of the P1 voltage for drug-free conditions and during exposure to five concentrations of drug (see symbol key). The dotted line shows least-squares fits of the data at each concentration of drug to the Boltzmann equation ($I = I_{max}/(1 + \exp[(V - V_{1/2})/k])$, where I_{max} is the maximum Na current measured at any given drug concentration, $V_{1/2}$ is the membrane potential where the channel availability is reduced by 50%, and k is a slope factor. The small current reduction in the first lidocaine concentration (2.6 μM) is ascribed to run-down commonly observed in the early experimental period, and not to higher-affinity rested-state block (also in Fig. 6). (*B*) The difference between the fitted $V_{1/2}$ at each drug concentration and the control $V_{1/2}$ ($V_{1/2}$ *shift*) measured in the same oocyte is plotted as a function of the drug concentration. The data are taken from three oocytes that were each exposed to control solutions and five concentrations of drug. A nonlinear function (Eq. 2) was fitted to these data (*dotted line*) to estimate K_R and K_{IF}. The resulting fitted parameters are shown on the figure and described in the text.

tions of α + β_1 in Fig. 1 *C*). In contrast, increasing the magnitude of k_2 and k_3 could provide mode 2 gating behavior. Channels in I_F can either reopen, causing bursts, or, alternatively, progress to I_S, causing slow inactivation after short depolarizations. The proposed increases in k_2 and k_3 amount to a simple destabilization of the fast-inactivated state during mode 2 gating. This model is attractive because it economically accounts both for bursting and for accelerated entry into the slow-inactivated state.

Transition between these gating modes would influence the time-dependent manner in which the fast- and slow-inactivated states are populated; however, the affinity of I_F and I_S after a prolonged depolarization may be approximated using steady-state assumptions that are consistent with this gating scheme (Eq. 3b) but do not incorporate the rate constants controlling movement between the drug-free states explicitly.

$$\begin{array}{ccccc} R & \rightleftharpoons & O & \rightleftharpoons & I_F \rightleftharpoons I_S \\ \updownarrow & & \updownarrow & & \updownarrow \quad \updownarrow \\ RL & & & & I_F L \quad I_S L \end{array} \qquad (3b)$$

Using this model, the $V_{1/2}$ shift can be expressed (see Appendix) as a function of the lidocaine concentration [*L*], the affinity of lidocaine for the rested (*R*), fast-inactivated (I_F), and slow-inactivated (I_S) states, and the relative occupancy of I_S to I_F ($[I_S]/[I_F]$) at steady state as follows:

$$V_{1/2}\ \text{shift} = k\ln\{(1 + L/K_R)(1 + [I_S]/[I_F])$$
$$[1 + L/K_{IF} + ([I_S]/[I_F])(1 + L/K_{IS})]^{-1}\}. \qquad (4)$$

The values for k, K_{IF}, and K_R were previously determined (Fig. 5 *B*), leaving I_S/I_F and K_{IS} as the only unknown parameters in Eq. 4. In repriming experiments with oocytes expressing α-alone channels where 5-s prepulses to −20 mV were used (not shown), we found that the ratio of slowly recovering current to rapidly recovering current was ~9:1.

A set of experiments similar to Fig. 5 *A* was performed with oocytes expressing α subunits alone to assess the affinity of lidocaine for slow-inactivated channels. To increase occupancy of the slow-inactivated state, the inactivating clamp steps (*P1*) were lengthened to 5 s. Fig. 6 *A* shows the results from a representative oocyte exposed to five incremental concentrations of lidocaine, with measurements at each lidocaine concentration fitted separately to the Boltzmann equation. Fig. 6 *B* shows the dependence of the drug-induced $V_{1/2}$ shift on lidocaine concentration. Using $I_S/I_F = 9$ in Eq.

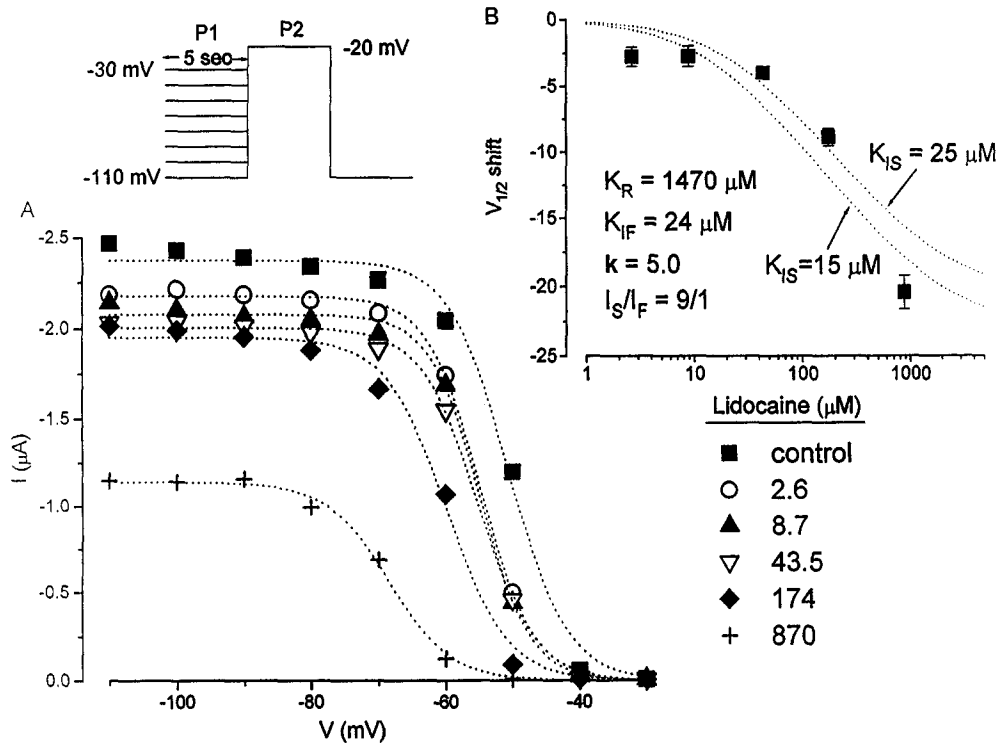

FIGURE 6. Steady-state block of slow-inactivated Na channels. Oocytes expressing α subunits without β_1 were subjected to a voltage-clamp protocol similar to that used in Fig. 5, except the inactivating clamp steps (*P1*) were lengthened to 5 s. (*A*) Peak Na currents from a representative oocyte exposed to the same incremental concentrations of lidocaine as in Fig. 5. The dotted lines show least-squares fits to the Boltzmann equation. (*B*) $V_{1/2}$ shift as a function of lidocaine concentration. The data are taken from three oocytes that were each exposed to control solutions and five concentrations of drug. The dotted lines show the predicted $V_{1/2}$ shift–concentration relationship predicted by Eq. 4. Values of K_{IS} ranging from 15 to 25 μM provide a reasonable fit to the data. Fixed values were used for K_R, K_{IF}, k, and I_S/I_F as indicated in the figure (see text).

4, we calculated the $V_{1/2}$ shift–concentration relationship for a range of K_{IS} values (Fig. 6 *B*, *dotted lines*). Simulations with K_{IS} values of 15 and 25 μM are shown; these yield plausible upper- and lower-limit estimates for the affinity of lidocaine for I_S. Using this expanded model, the shape of the 25-μM fitted line is not dramatically altered from Fig. 5 *B*. This suggests that, while the rate of recovery from block of I_S may be slower than that of recovery from I_F (Fig. 2 *B*), the affinity of the two inactivated states for lidocaine may be similar.

As a consistency check on this model-dependent method for determining the slow-inactivated state affinity, we modified our approach and used a model-independent analysis. In Fig. 7 *A*, peak Na currents in the presence of lidocaine were replotted as a fraction of the control current over a range of prepulse potentials from −110 to −50 mV. Currents elicited by test pulses (*P2*) after prepulse potentials (*P1*) positive to −50 mV were too small to measure drug effects reliably. The mean peak current values at each voltage were fitted to a logistic function (see legend) to determine the ED_{50} for drug binding at each potential. At −110 mV, the fitted ED_{50} for lidocaine-induced reduction of current was 2,480 μM. The K_R in the absence of β_1 determined in this way is higher than the previously determined model-dependent estimate (1,470 μM); however, the model-independent value should be viewed as approximate since drug concentrations >1 mM were not used. As the prepulse potentials were progressively depolarized from −110 to −50 mV, the ED_{50} decreased nonlinearly to 92 μM. Even at the most depolarized potential used, a significant fraction of channels remain in the rested, low-affinity state (see control data in Fig. 6 *A*, only ~50% inactivation at −50 mV); thus, the fit to the peak current ratio (Fig. 7 *A*) represents an underestimate of the slow-inactivated state affinity. Fig. 7 *B* plots the ED_{50}–voltage relationship in a semilog format. The dotted horizontal lines indicate the previous model-dependent prediction for K_{IS} at −20 mV. Although no simple analytical relationship can be fitted to these data, the decline in the ED_{50} with depolarization has clearly not saturated at −50 mV, suggesting that K_{IS} is significantly smaller than 92 μM.

Open-Channel Block by Lidocaine

Our preceding analysis of lidocaine block ignores the potential contribution of lidocaine binding to the open channel (Eq. 1 and 3). In view of the probable enhancement of mode 2 bursting in the absence of β_1 (Zhou et al., 1991), channels are likely to spend more time in the open state and therefore may exhibit en-

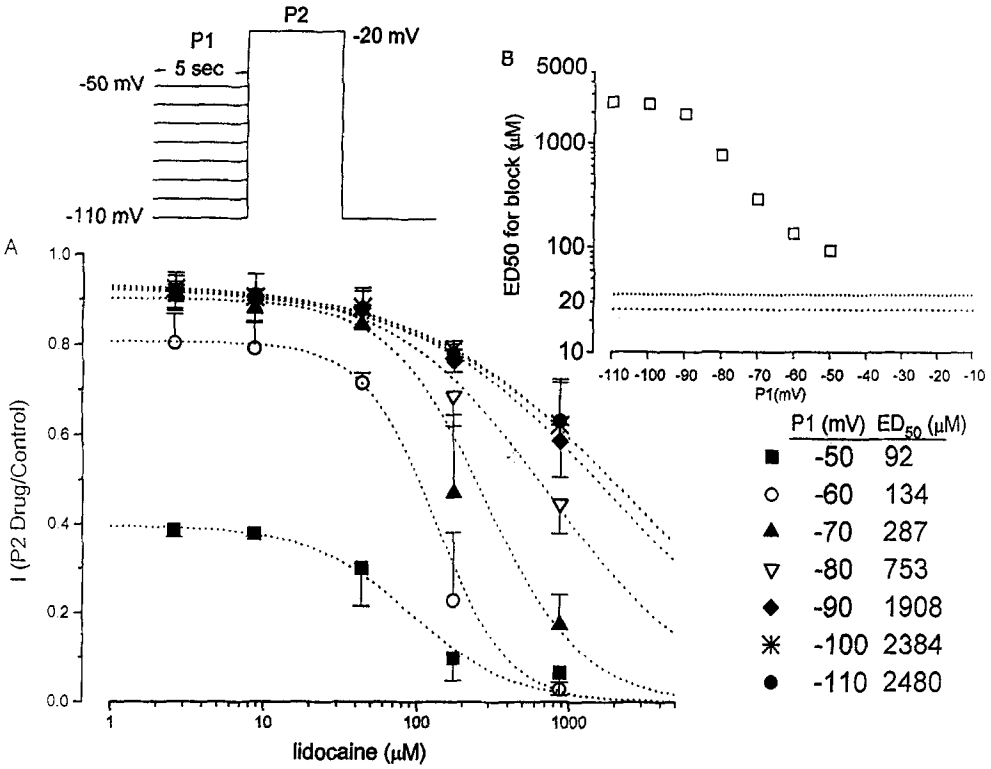

FIGURE 7. Model-independent assessment of slow-inactivated channel affinity for lidocaine. (*A*) Peak Na currents in lidocaine were replotted (from Fig. 6) as a fraction of the control current measured in the same oocyte; summary data from three oocytes are shown. The mean values at each voltage were fitted to a logistic function $y = y_{max}/[1 + (ED_{50}/D)^P]$, where ED_{50} is the drug concentration reducing the current by 50%, D is the drug concentration, and P is the slope factor. The fitted ED_{50} values are shown on the figure at each membrane potential in tabular form. (*B*) ED_{50} values from *A* are plotted as a function of prepulse (*P1*) membrane potential. The ED_{50}–voltage relationship declines with depolarization and has not reached a plateau by −50 mV. The minimum ED_{50} measured was 92 μM at −50 mV, a membrane potential where a significant fraction of channels were still in the lower-affinity *R* (rested) state. The dotted lines indicate the 15–25 μM K_{IS} values determined from the model-dependent analysis in Fig. 6 *B*.

hanced block based on this difference alone. Analysis of lidocaine effects on single cardiac Na channels in guinea pig ventricular cells indicates that there is no reduction in single-channel current amplitude, inconsistent with a substantial rapid open-channel block component. However, a significant reduction in channel open time was seen with lidocaine, as well as nearly total elimination of open-channel bursting (Nilius et al., 1987). The influence of open-channel block on our results was examined by comparing α-alone (Fig. 8) currents in the absence and presence of lidocaine (paired observations); the area under the current trace (Fig. 8 *B*) and the time from peak current to 50% decay (Fig. 8 *C*) were taken as indices of total open-channel probability. Both analyses revealed a small, statistically insignificant reduction due to lidocaine that could not explain the substantial delays in repriming seen in the absence of β_1.

DISCUSSION

The complex frequency- and voltage-dependent features of local anesthetic block of voltage-gated Na channels have been rationalized by models that link receptor affinity to the conformational state of the channel (Hille, 1977; Hondeghem and Katzung, 1977). The use dependence of local anesthetic block suggests that inactivated states have high drug affinity and that unbinding of local anesthetics occurs during hyperpolarization as the channels assume a lower affinity rested-state conformation. Enzymatic removal of fast inactivation by exposure of the cytoplasmic membrane surface to protease attenuates use-dependent Na channel block by quaternary amine compounds (Cahalan, 1978; Yeh, 1978). However, for the tertiary amine compounds etidocaine and tetracaine, a substantial component of use-dependent block remained after pronase treatment (Cahalan, 1978), suggesting the possibility that these compounds may bind tightly to additional domains or conformational states of the channel.

The Character of Slow Inactivation in Na Channels Expressed from α Subunits Alone

Our analysis of the large, slow recovery component seen in oocytes expressing α subunits expressed alone is predicated on the belief that this kinetic state is fundamentally similar, if not identical, to the slowly recovering state seen in vivo after prolonged depolarizations (Rudy, 1978). In *Xenopus* oocytes (Zhou et al., 1991) and HEK cells (Ukomadu et al., 1992), at least two kinetic components are seen in whole-cell and single-channel experiments with α subunit expressed alone. A predominant gating mode (mode 1) was identified that

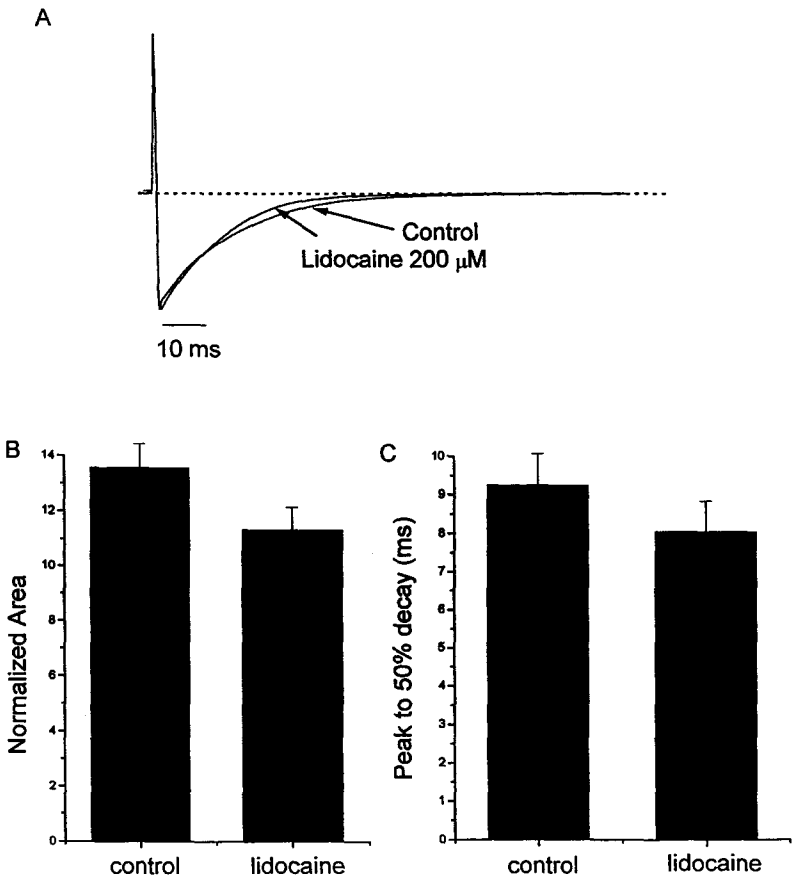

FIGURE 8. Analysis of the magnitude of open-channel block during depolarization in α subunits expressed alone. (*A*) Normalized whole-cell (α-alone) currents at −20 mV (from a −100-mV holding potential) recorded from the same oocyte in control conditions and after lidocaine addition to the bath. Currents were not leak subtracted. The current decay in lidocaine appears to be slightly accelerated. (*B*) The area between the normalized current trace and the zero current abscissa (AUC) before and during lidocaine (175 μM) exposure in oocytes expressing α subunits alone (n = 5, paired). Total AUC was reduced from 13.5 ± 0.9 to 11.3 ± 0.8 (P = 0.11). (*C*) In the same five oocytes, time from peak to 50% current decay was 9.2 ± 0.8 in control conditions and 8.0 ± 0.8 in lidocaine (P = 0.33).

consisted mostly of single openings with ensemble average kinetics consistent with the fast component of whole-cell current decay. A less prominent slow gating mode (mode 2), characterized by bursts of reopenings during depolarization, may underlie the slower of the two kinetic components in the decay of macroscopic current. Single-channel analysis of mode 2 gating in *Xenopus* indicates that mode 2 bursting channels frequently lapse into a long periods of quiescence, which may contribute to the slow recovery phenomena seen in whole-cell experiments (Ukomadu et al., 1992; Zhou et al., 1991). It was noted that the voltage dependence of the slow decay component in HEK cells was similar to that measured in oocytes, and the bursting behavior of mode 2 channels in HEK cells was found to "closely resemble" the mode 2 gating observed in oocytes (Ukomadu et al., 1992). This suggested that the slow decay component observed in oocytes, while prominent, displays properties similar to those seen in mammalian cells. Further, when non-α subunit cRNAs were coinjected into *Xenopus* oocytes, the amplitude of the slow component of decay was reduced, but its time constant did not change, and in single-channel experiments with coinjected oocytes, the two gating modes persisted with unaltered time constants (Zhou et al., 1991). Hence, β_1 coexpression in oocytes does not appear to alter the kinetic features of slow gating, just its prominence.

Although studies (Ukomadu et al., 1992; Zhou et al., 1991) discuss a potential link between occupancy of a slowly recovering state, mode 2 bursting behavior, and slow decay of whole-cell current, the experimental data do not exclude the possibility that mode 1 channels may slow inactivate. As shown in Fig. 1 *C*, during prolonged depolarization, α + β_1 channels exhibited significant slow inactivation (~30% of the channels recovered slowly after 2-min depolarizing steps). It is unlikely that α + β_1 channels exhibit substantial mode 2 bursting under these conditions, and we have found no measurable plateau of noninactivating inward current during prolonged depolarizations in whole-cell experiments. The agreement between the rate of slow recovery for α + β_1 coexpressed channels after long depolarizations and α-alone channels after brief depolarizations (Fig. 1, *B* and *C*) thus provides additional evidence that (*a*) channels gating in the fast mode may slow inactivate, and (*b*) the slow-inactivated state, once occupied, is kinetically similar for α + β_1 and α-alone channels. The assumption that channels in either mode may slow inactivate is an implicit assumption in our model for steady-state block of α-alone channels by lidocaine (Eq. 3b).

Slow-inactivated Na Channels Exhibit Ultra-slow Recovery from Lidocaine Block

By using μ1 Na channel α subunits expressed without the subsidiary β_1 subunit, we have demonstrated an additional high-affinity (K_d = 15–25 μM, Figs. 6 and 7) component of lidocaine block that appears to be linked to slow inactivation. Slow-inactivated channels recovered much more slowly from block than did fast-inactivated channels (Fig. 2 *B*). Ultra-slow recovery from inactivated-state block was identified in early voltage-clamp studies of local anesthetics and was initially interpreted as a kinetically silent slow-inactivated state induced by drug binding (Khodorov et al., 1976). In contrast, Hille suggested that ultra-slow recovery of blocked, inactivated channels is a consequence of slow departure of drug from the inactivated channel via the hydrophobic pathway, and not a consequence of binding to a distinct slow-inactivated state (Hille, 1977). Our results comparing the recovery of channels that primarily exhibit fast inactivation (α + β_1) with channels that develop substantial slow inactivation (Fig. 2 *B*, α *alone*) suggest that both viewpoints may be correct. Recovery of fast-inactivated channels from lidocaine block is significantly slower than recovery from fast inactivation but clearly faster than recovery of drug-blocked slow-inactivated channels.

A similar reduction in use-dependent lidocaine block has been linked to β_1 coexpression with cardiac Na channel α subunits (hH1) (Makielski et al., 1995). Because no significant β_1 effects on the rate of hH1 inactivation were observed, it was proposed that β_1 acts directly at the local anesthetic binding site. However, results from our laboratory (Nuss et al., 1995*a*) indicate that β_1 accelerates inactivation and recovery from inactivation of hH1 channels expressed in *Xenopus* oocytes. Thus, we favor an alternate interpretation for the effects of β_1 on use-dependent block. We propose that β_1 reduces the probability of slow inactivation during short (50-ms) depolarizations, and consequently reduces the probability of slow-inactivated channel block. Since recovery from slow-inactivated channel block is slower than recovery from fast-inactivated channel block (Fig. 2 *B*), use-dependent block is attenuated in the presence of the β_1 subunit.

Structure–Function Correlations for Slow-inactivated Channel Block

Site-directed mutagenesis of expressed Na channels has linked fast inactivation to hydrophobic cytoplasmic residues between domains III and IV (West et al., 1992), and lidocaine block of expressed Na channels is modified by mutation of these cytoplasmic residues (Lawrence et al., 1993; Bennett et al., 1995). In contrast, the structure–function relationships defining slow inactivation of Na channels have not been described. Accordingly, the structural features that define the interaction between slow-inactivated channels and local anesthetics are similarly unclear. However, in potassium channels, mutagenesis studies have linked slow inactivation to structural elements in the external pore region separate from the cytoplasmic fast inactivation gating apparatus (Choi et al., 1991; Hoshi et al., 1991; Yellen et al., 1994). Similarly, internal treatment of squid axons with pronase effectively removed fast inactivation but did not remove the slow recovery component (Rudy, 1978). Our experiments with Na channels genetically modified in the III-IV linker to remove fast inactivation (IFM/QQQ) also confirm that both slow decay and slow recovery from inactivation are retained (data not shown). We have also shown that an external pore-lining residue in domain I (W402) has profound effects on inactivation gating (Tomaselli et al., 1995). Although the influence of this residue on lidocaine block is as yet undetermined, other residues in domain IV that may face the pore have been implicated in use-dependent local anesthetic block of rat brain IIA Na channels (Ragsdale et al., 1994).

Single-channel studies suggest that local anesthetics bind deep within the pore, perhaps as far as 70% into the membrane field from the cytoplasmic side (Gingrich et al., 1993). If pore-lining residues are critical for slow inactivation in Na channels, as they are in K channels (Choi et al., 1991; Hoshi et al., 1991; Yellen et al., 1994), it is reasonable to propose an interaction between drug binding and slow inactivation. Consistent with this idea, a paradigm for drug association with fast- and slow-inactivated channels in native tissue is diagrammatically illustrated in Fig. 9. During brief depolarizations, channels would open and fast inactivate. Upon hyperpolarization of the membrane, recovery from inactivation would be rapid. In contrast, during long depolarizations (e.g., ischemic tissue), channels would develop slow inactivation; recovery from slow inactivation upon hyperpolarization would also be slow. In the presence of drug, brief depolarizations would induce the fast-inactivated blocked state, from which recovery is slow. More prolonged depolarization would induce an even more stable, drug-associated state, possibly because of a conformational change in the external pore region during slow inactivation. Such channels would exhibit ultra-slow recovery from block (>10 s) because of the stability of the local anesthetic association with the slow-inactivated channel conformation. Although not shown in Fig. 9, our analysis (Eqs. 3 and 4; Fig. 6 *B*) suggests that a significant fraction of channels would also recover slowly from fast-inactivated channel block after long depolarizations.

Our data suggest that a significant fraction of blocked channels, when expressed in the absence of β_1, slow in-

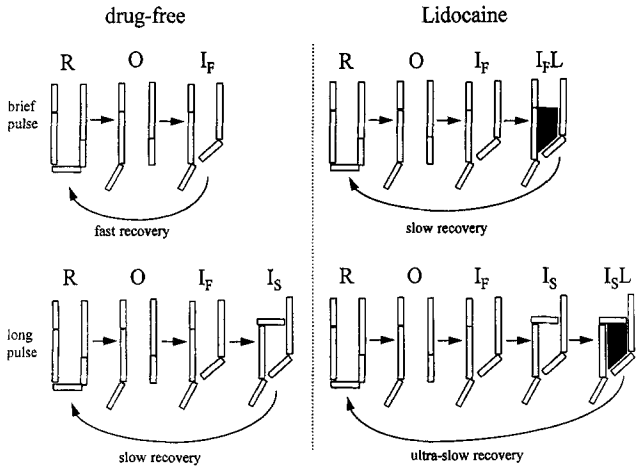

FIGURE 9. A model that illustrates possible interactions between lidocaine (*L*) and channels that are fast and slow inactivated. Rightward arrows indicate transitions that occur during depolarization after drug enters the open channel, and leftward arrows indicate the recovery processes during repolarization. The states are highly diagrammatic and are intended to show how the channel conformation may influence block. (*Top, left*) In the absence of drug during brief depolarizations (e.g., action potentials in nonischemic tissue), channels leave the rested state (*R*) and transiently enter the open state (*O*) before they fast inactivate (I_F). Upon hyperpolarization of the membrane, recovery from inactivation would be rapid (fast recovery). (*Bottom, left*) In contrast, during long depolarizations (e.g., ischemic tissue) in the absence of drug, channels would fast inactivate and then slow inactivate (I_S). Upon repolarization, recovery from the slow-inactivated state would also be slow. (*Top, right*) In the presence of drug, brief depolarizations would induce the fast-inactivated, blocked state (I_FL), from which recovery is slow. (*Bottom, right*) Prolonged depolarization in the presence of drug would allow formation of a stable, drug-associated slow-inactivated state (I_SL). I_SL channels would exhibit ultra-slow recovery from block (>10 s) because of the stability of the local anesthetic association with the slow-inactivated channel conformation.

activate even during short depolarizations (Fig. 2 *B*). In the model (Fig. 9), these channels slow inactivate after first fast inactivating; that is, slow-inactivated channels may retain some of the structural features of fast-inactivated channels. Although our data provide no direct evidence to suggest that Na channels inactivate sequentially in this manner, the idea is not original. A comprehensive analysis of Na channel gating currents during fast and slow inactivation suggested this possibility (Bezanilla et al., 1982), as did earlier studies of inactivated-channel block (Khodorov et al., 1976). Although single-channel experiments have suggested a linkage between mode 2 bursting behavior and occupancy of slow-inactivated states (Zhou et al., 1991), these data do not exclude the possibility that mode 1 channels, after first fast inactivating, may slow inactivate. In fact, studies on *Shaker* potassium channels with part of their amino terminus deleted indicate that the slower, C-type inactivation occurs most readily from N-type inactivated states (Hoshi et al., 1991). If slow-inactivated channels retain the essential features of fast inactivation (e.g., III-IV linker binding in the pore), it is possible that the structural features of both fast and slow inactivation may be required for slow-inactivated channel block. In support of this idea, slow-inactivated hH1 Na channels were not blocked by lidocaine when fast inactivation was eliminated by the III-IV linker IFM/QQQ mutation (Bennett et al., 1995).

Coexpression of β_1 increases the occupancy of fast-inactivated states relative to slow-inactivated states during depolarization in *Xenopus* oocytes (Fig. 1 *B*) but does not significantly alter the rate of recovery from fast inactivation (Fig. 2 *B*) or fast-inactivated channel block (Fig. 3 *B*). Thus, the β_1 subunit appears to inhibit formation of the slow-inactivated state in oocytes without altering the kinetics of fast inactivation. This finding may suggest that channel regions involved in the interaction between the slow-inactivated state and the β_1 subunit are distant from the fast-inactivation gate. The topology of the rat brain Na channel β_1 subunit includes a single membrane-spanning segment, a glycosylated extracellular domain, and virtually no cytoplasmic segment (Isom et al., 1992). It seems unlikely that β_1 subunit affects the fast inactivation mechanism directly but instead inhibits progression of fast-inactivated channels to the slow-inactivated state. As a result, the majority of $\alpha + \beta_1$ channels remain in the fast-inactivated blocked state and upon repolarization undergo slow, but not ultra-slow, recovery from block. While we find this scheme intuitively attractive, other mechanisms that invoke nonsequential models for the fast- and slow-inactivated conformations cannot be excluded on the basis of our data.

Estimates of Inactivated-State Affinity

In previous work, the model-independent method shown in Fig. 7 was used to assess the affinity of fast-inactivated $\alpha + \beta_1$ channels for lidocaine (Nuss et al., 1995*b*). Since long depolarizing prepulses (minutes) were used, the relative contribution of fast and slow inactivation to the measurement is uncertain; however, the K_I of 12 μM is similar to our measurements for K_{IF} (24 μM) and K_{IS} (15–25 μM) using model-dependent methods (Figs. 5 and 6). Bean et al. (1983) noted a similar K_I of 10 μM for lidocaine in native cardiac channels using both model-dependent and model-independent techniques. Our $V_{1/2}$ shift-concentration data from $\alpha + \beta_1$ channels after short (500-ms) prepulses were well described by the same model with a single inactivated state (Eqs. 1 and 2). When attempting to fit the data from α-alone channels after long depolarizations (5 s),

we considered the possibility that both fast and slow inactivation would influence the steady-state dose-response curves of α-alone channels. When the contribution of lidocaine binding to a slow-inactivated state (Eqs. 3 and 4, also see Appendix) was included, we were able to obtain good agreement between the model and the data using K_{IS} values of 15–25 μM (Fig. 6 *B*), suggesting that the affinity of the fast- and slow-inactivated states for lidocaine are similar. This result is consistent with Bean et al. (1983), where the lidocaine-induced $V_{1/2}$ shift in inactivation (h_∞) after long pulses (>10 s) was simulated with a single inactivated state (see Fig. 7 from Bean et al., 1983). Hence, whereas slow inactivation strongly influences the rate of recovery from inactivated-channel block (Fig. 2 *B*), the steady-state effects of lidocaine on the h_∞ curve are similar to those of the fast-inactivated channel.

Pharmacologic Significance of the β_1 Subunit

While it is certain that the β_1 subunit modulates Na channel gating in *Xenopus* oocytes, the importance of this effect in mammalian expression systems is less clear. Coexpression of β_1 in mammalian cells has subtle effects on Na channel gating compared with the changes seen in *Xenopus* oocytes (Scheuer et al., 1990; Isom et al., 1995). The absence of an endogenous β_1 subunit in mammalian cells typically used for channel expression suggests that the differences in the β_1 effect relate to differences in posttranslational modification or protein–protein interactions (Isom et al., 1995). The modulatory role of β_1 subunit with regard to local anesthetic block in native cells is unknown. However, slow-inactivated states are likely to assume critical pharmacologic importance in tissues subjected to prolonged depolarization (e.g., ischemia). Therefore, the value of β_1 modulation of Na channel α subunits expressed in *Xenopus* oocytes rests in facilitating the simultaneous examination of the fast- and slow-inactivated states and their unique pharmacological properties.

APPENDIX

The state model (Eq. 3b) considered for a channel that may sequentially enter two inactivated states, I_F and I_S, and bind lidocaine [L] in either of those states or the rested state (R) is as follows:

$$\begin{array}{ccccc} R & \rightleftharpoons & O & \rightleftharpoons & I_F \\ K_R \updownarrow & & K_{IF} \updownarrow & & \updownarrow K_{IS}. \\ RL & & I_FL & & I_SL \end{array} \qquad \begin{array}{c} \rightleftharpoons I_S \\ \\ \\ \end{array}$$

We have assumed that the open state (O) is transiently occupied and does not influence steady-state block after long prepulses. K_R, K_{IF}, and K_{IS} are the affinities of lidocaine for the rested, fast-inactivated, and slow-inactivated states, respectively, where

$$L \cdot [R] = K_R \cdot [RL] \tag{A1}$$

$$L \cdot [I_F] = K_F \cdot [I_FL] \tag{A2}$$

$$L \cdot [I_S] = K_S \cdot [I_SL]. \tag{A3}$$

The square brackets indicate fractional occupancy, and L is the lidocaine concentration. The availability of channels to open at any given membrane potential reflects occupancy of the rested state [R]. Because the I_F and I_S states are absorbing, [R] decreases as the membrane potential is depolarized. The membrane potential at which 50% of the channels are available to open ($V_{1/2}$) is used as an index of channel availability to open under specified experimental conditions; $V_{1/2}$ may be left shifted by lidocaine because of its high inactivated-state affinity. We wish to obtain an expression for $V_{1/2}$ as a function of lidocaine concentration and lidocaine affinity for the R, I_F, and I_S states.

The expression for occupancy of R as a function of voltage may be written as follows:

$$[I_F]/[R] = \exp[(V - V_o)/k], \tag{A4}$$

where k is the Boltzmann slope that incorporates the requisite energy terms, V is the membrane potential, and V_o is the membrane potential when $R = I_F$. Note that when more than two states are present, V_o is not necessarily $V_{1/2}$.

The total occupancy must equal unity; hence,

$$[R] + [RL] + [I_F] + [I_FL] + [I_S] + [I_SL] = 1. \tag{A5}$$

By substituting Eqs. A1–A3 into Eq. A5, we obtain

$$[R](1 + L/K_R) + [I_F](1 + L/K_{IF}) + [I_S](1 + L/K_{IS}) = 1 \tag{A6}$$

$$[R](1 + L/K_R) + [I_F][(1 + L/K_{IF}) + ([I_S]/[I_F])(1 + L/K_{IS})] = 1. \tag{A7}$$

Occupancy of R is maximal when $[I_F] = 0$; hence,

$$[R]_{max} = (1 + L/K_R)^{-1}. \tag{A8}$$

Occupancy of R is half-maximal when

$$[R] = [R]_{max}/2 = 1/2\,(1 + L/K_R)^{-1} \tag{A9}$$

Substituting Eq. A9 into Eq. A7 and solving for I_F gives the following simplified expression when [R] is half-maximal:

$$[I_F] = 1/2\,[(1 + L/K_{IF}) + ([I_S]/[I_F])(1 + L/K_{IS})]^{-1}. \tag{A10}$$

Substituting Eqs. A9 and A10 for the occupancy of I_F and R when $[R] = [R]_{max}/2$ into the Boltzmann expression (Eq. A4) gives (after simplification)

$$V \text{ at } [R]_{max}/2 = k\ln\{(1 + L/K_R)$$
$$[1 + L/K_{IF} + [I_S]/[I_F](1 + L/K_{IS})]^{-1}\} - V_o. \quad (A11)$$

Finally, the $V_{1/2}$ shift due to lidocaine at a given drug concentration may be obtained from the difference equation as follows:

$$V_{1/2} \text{ shift} = V \text{ at } [R]_{max}/2 \text{ when } L \neq 0$$
$$- (V \text{ at } [R]_{max}/2 \text{ when } L = 0). \quad (A12)$$

Substituting Eq. A11 into Eq. A12 and simplifying gives Eq. 4:

$$V_{1/2} \text{ shift} = k\ln\{(1 + L/K_R)(1 + [I_S]/[I_F])$$
$$[1 + L/K_{IF} + ([I_S]/[I_F])(1 + L/K_{IS})]^{-1}\}.$$

In the absence of slow inactivation (see Eq. 1), $[I_S]/[I_F] = 0$. Using this simplification, an expression for the $V_{1/2}$ shift for the case of one inactivated state may be written (Eq. 2; also see Bean et al., 1983)

$$V_{1/2} \text{ shift} = k\ln[(1 + [L]/K_R)(1 + [L]/K_{IF})^{-1}].$$

This work was supported by National Institutes of Health grants R01HL50411 (G.F. Tomaselli) and R01HL52307 (E. Marban); American Heart Association (AHA), Maryland Affiliate (H.B. Nuss); AHA-Clinician Scientist Award and the Passano Clinician Scientist Award of the Johns Hopkins School of Medicine (J.R. Balser).

Original version received 18 September 1995 and accepted version received 15 February 1996.

REFERENCES

Adelman, W.J., and Y. Palti. 1969. The effects of external potassium and long duration voltage conditioning on the amplitude of sodium currents in the giant axon of the squid, *Loligo pealei*. *J. Gen. Physiol.* 54:589–606.

Backx, P.B., D.T. Yue, J.H. Lawrence, E. Marban, and G.F. Tomaselli. 1992. Molecular localization of an ion-binding site within the pore of mammalian sodium channels. *Science (Wash. DC).* 257:248–251.

Bean, B.P., C.J. Cohen, and R.W. Tsien. 1983. Lidocaine block of cardiac sodium channels. *J. Gen. Physiol.* 81:613–642.

Bennett, P.B., N. Makita, and A.L. George. 1993. A molecular basis for gating mode transitions in human skeletal muscle sodium channels. *FEBS Lett.* 326:21–24.

Bennett, P.B., C. Valenzuela, C. Li-Qiong, and R.G. Kallen. 1995. On the molecular nature of the lidocaine receptor of cardiac Na^+ channels. *Circ. Res.* 77:584–592.

Bezanilla, F., R.E. Taylor, and J.M. Fernandez. 1982. Distribution and kinetics of membrane dielectric polarization: long-term inactivation of gating currents. *J. Gen. Physiol.* 79:21–40.

Cahalan, M.D. 1978. Local anesthetic block of sodium channels in normal and pronase-treated squid axons. *Biophys. J.* 23:285–311.

Cannon, S.C., A.I. McClatchey, and J.F. Gusella. 1993. Modification of the Na^+ current conducted by the rat skeletal muscle α subunit by coexpression with a human brain β subunit. *Pflügers Arch. Eur. J. Physiol.* 423:155–157.

Chandler, W.K., and H. Meves. 1970. Slow changes in membrane permeability and long lasting action potentials in axons perfused with fluoride solutions. *J. Physiol. (Camb.).* 211:707–728.

Choi, K.L., R.W. Aldrich, and G. Yellen. 1991. Tetraethylammonium blockade distinguishes two inactivation mechanisms in voltage-activated K^+ channels. *Proc. Natl. Acad. Sci. USA.* 88:5092–5095.

Courtney, K.R. 1975. Mechanism of frequency-dependent inhibition of sodium currents in the frog myelinated nerve by the lidocaine derivative gea 968. *J. Pharmacol. Exp. Ther.* 195:225–236.

Gingrich, K.J., D. Beardsley, and D.T. Yue. 1993. Ultra-deep blockade of Na channels by a quaternary ammonium ion: catalysis by a transition-intermediate state? *J. Physiol. (Camb.).* 471:319–341.

Hille, B. 1977. Local anesthetics: hydrophilic and hydrophobic pathways for the drug-receptor reaction. *J. Gen. Physiol.* 69:497–515.

Hodgkin, A.L., and A.F. Huxley. 1952. A quantitative description of membrane current and its application to conduction and excitation in nerve. *J. Physiol. (Camb.).* 117:500–544.

Hondeghem, L.M., and B.G. Katzung. 1977. Time- and voltage-dependent interactions of the antiarrhythmic drugs with cardiac sodium channels. *Biochim. Biophys. Acta.* 472:373–398.

Hoshi, T., W.N. Zagotta, and R.W. Aldrich. 1991. Two types of inactivation in *Shaker* K^+ channels: effects of alterations in the carboxy-terminal region. *Neuron.* 7:547–556.

Isom, L.L., K.S. Dejongh, D.E. Patton, B.F.X. Reber, J. Offord, H. Charbonneau, K. Walsh, A.L. Goldin, and W.A. Catterall. 1992. Primary structure and functional expression of the beta-1 subunit of the rat brain sodium channel. *Science (Wash. DC).* 256: 839–842.

Isom, L.L., T. Scheuer, A.B. Brownstein, D.S. Ragsdale, B.J. Murphy, and W.A. Catterall. 1995. Functional co-expression of the β1 and type IIA α subunits of sodium channels in a mammalian cell line. *J. Biol. Chem.* 270:3306–3312.

Khodorov, B., L. Shishkova, E. Peganov, and S. Revenko. 1976. Inhibition of sodium currents in frog Ranvier node treated with local anesthetics: role of slow sodium inactivation. *Biochim. Biophys. Acta.* 433:409–435.

Lawrence, J.H., H.B. Nuss, R.H. Xu, E. Marban, and G.F. Tomaselli. 1993. Mechanism of antiarrhythmic drug binding: insights from lidocaine block of inactivation-deficient mutant sodium channels. *Clin. Res.* 41:143*a*. (Abstr.)

Makielski, J.C., A. Alpert, and D.A. Hanck. 1991. Two components of use-dependent block of sodium current by lidocaine in voltage clamped purkinje cells. *J. Mol. Cell. Cardiol.* 23(Suppl. I):95–102.

Makielski, J.C., J.T. Limberis, S.Y. Chang, Z. Fan, and J.W. Kyle.

1995. Na channel β_1 association with cardiac Na channel α subunits demonstrated by lidocaine block. *Biophys. J.* 68:157*a*. (Abstr.)

Matsubara, T., C. Clarkson, and L. Hondeghem. 1987. Lidocaine blocks open and inactivated cardiac sodium channels. *Naunyn-Schmiedeberg's Arch. Pharmacol.* 336:224–231.

Moorman, J.R., G.E. Kirsch, A.M.J. VanDongen, R.H. Joho, and A.M. Brown. 1990. Fast and slow gating of sodium channels encoded by a single mRNA. *Neuron.* 4:243–252.

Nilius, B., K. Benndorf, and F. Markwardt. 1987. Effects of lidocaine on single cardiac sodium channels. *J. Mol. Cell. Cardiol.* 19:865–874.

Nuss, H.B., N. Chiamvimonvat, M.T. Perez-Garcia, G.F. Tomaselli, and E. Marban. 1995*a*. Functional association of the β_1 subunit with human cardiac (hH1) and rat skeletal muscle (μ1) sodium channel α subunits expressed in *Xenopus* oocytes. *J. Gen. Physiol.* 106:1171–1191.

Nuss, H.B., G.F. Tomaselli, and E. Marban. 1995*b*. Cardiac sodium channels (hH1) are intrinsically more sensitive to tonic block by lidocaine than are skeletal muscle (μ1) channels. *J. Gen. Physiol.* 106:1193–1210.

Patlak, J. 1991. Molecular kinetics of voltage-dependent Na^+ channels. *Physiol. Rev.* 71:1047–1080.

Ragsdale, D.S., J.C. McPhee, T. Scheuer, and W.A. Catterall. 1994. Molecular determinants of state-dependent block of Na^+ channels by local anesthetics. *Science (Wash. DC).* 265:1724–1728.

Rudy, B. 1978. Slow inactivation of the sodium conductance in squid giant axons. Pronase resistance. *J. Physiol.* 238:1–21.

Scheuer, T., V.J. Auld, S. Boyd, J. Offord, R. Dunn, and W.A. Catterall. 1990. Functional properties of rat brain sodium channels expressed in a somatic cell line. *Science (Wash. DC).* 247:854–858.

Tomaselli, G.F., N. Chiamvimonvat, H.B. Nuss, J.R. Balser, M.T. Perez-Garcia, R.H. Xu, D.W. Orias, P.H. Backx, and E. Marban. 1995. A mutation in the pore of the sodium channel alters gating. *Biophys. J.* 68:1814–1827.

Ukomadu, C., J. Zhou, F.J. Sigworth, and W.S. Agnew. 1992. μ1 Na^+ channels expressed transiently in human embryonic kidney cells: biochemical and biophysical properties. *Neuron.* 8:663–676.

West, J., D. Patton, T. Scheuer, Y. Wang, A.L. Goldin, and W.A. Catterall. 1992. A cluster of hydrophobic amino acid residues required for fast Na^+-channel inactivation. *Proc. Natl. Acad. Sci. USA.* 89:10910–10914.

Yeh, J.Z. 1978. Sodium inactivation mechanism modulates qx-314 block of sodium channels. *Biophys. J.* 24:569–574.

Yellen, G., D. Sodickson, T. Chen, and M.E. Jurman. 1994. An engineered cysteine in the external mouth of a K^+ channel allows inactivation to be modulated by metal binding. *Biophys. J.* 66:1068–1075.

Zhou, J., J.F. Potts, J.S. Trimmer, W.S. Agnew, and F.J. Sigworth. 1991. Multiple gating modes and the effect of modulating factors on the μ1 sodium channel. *Neuron.* 7:775–785.